



Geophysical Research Letters°

S

RESEARCH LETTER

10.1029/2022GL101663

Key Points:

- A preexisting stratocumulus deck is more persistent when experiencing warm-air advection than cold-air advection
- This persistence is due to reduced entrainment drying as a result of decoupling, which outweighs decreased cloud-base moisture transport
- The mechanism is more notable when free-tropospheric humidity is higher

Supporting Information:

Supporting Information may be found in the online version of this article.

Correspondence to:

Z. Li and Y. Zheng, zhanqing@umd.edu; yzheng18@uh.edu

Citation:

Zhang, H., Zheng, Y., Lee, S. S., & Li, Z. (2023). Surface-atmosphere decoupling prolongs cloud lifetime under warm advection due to reduced entrainment drying. *Geophysical Research Letters*, 50, e2022GL101663. https://doi.org/10.1029/2022GL101663

Received 10 OCT 2022 Accepted 28 FEB 2023

© 2023. The Authors. This is an open access article under the terms of the Creative Commons Attribution License, which permits use, distribution and reproduction in any medium, provided the original work is properly cited.

Surface-Atmosphere Decoupling Prolongs Cloud Lifetime Under Warm Advection Due To Reduced Entrainment Drying

Haipeng Zhang¹, Youtong Zheng^{2,3}, Seoung Soo Lee^{1,4,5}, and Zhanqing Li¹

¹Department of Atmospheric and Oceanic Science & Earth System Science Interdisciplinary Center, University of Maryland, College Park, MD, USA, ²Program in Atmospheric and Oceanic Sciences, Princeton University, Princeton, NJ, USA, ³Department of Atmospheric and Earth Science, University of Houston, Houston, TX, USA, ⁴Science and Technology Corporation, Hampton, VA, USA, ⁵Research Center for Climate Sciences, Pusan National University, Busan, Republic of Korea

Abstract An initially well-mixed stratocumulus deck can remain overcast for several tens of hours under warm-advection conditions, although moisture supply is cut off from the ocean due to surface-atmosphere decoupling (stabilization of the surface-atmosphere interface). In this study, a set of idealized large-eddy simulations were performed to investigate the physical mechanism of how warm-air advection impacts the evolution of a pre-existing stratocumulus deck. To mimic warm-air advection, we decrease the sea surface temperature linearly over time in a doubly periodic domain. Given the same initial conditions, the stratocumulus deck is more persistent when experiencing warm-air advection than cold-air advection. This persistence is caused by reduced cloud-top entrainment drying due to decoupling, a process more influential than the decoupling-induced cutoff of moisture supply. This mechanism is more notable when the free troposphere becomes more humid. The relevance of the mechanism to previous observations of less low-level cloudiness under warm-advection conditions is discussed.

Plain Language Summary Marine stratocumulus clouds exert strong radiative cooling on Earth's climate because they reflect much solar radiation back to space. It is important to understand what factors control the cloud properties, or cloud-controlling factors. Among all cloud-controlling factors, the least understood is warm-air advection, meaning winds mobilizing clouds from over warm water to over cold water. A high-resolution numerical model was used to investigate the response of the stratocumulus evolution to warm-air advection. A stratocumulus deck was found to persist longer under warm-advection conditions than its cold counterpart, inconsistent with the decoupling-induced dissipation mechanism. This persistence is primarily due to the weaker mixing of clouds with the overlying dry air when the atmosphere become decoupled from the sea surface, a consequence of warm-air advection. This work revises our conventional understanding of how clouds respond to changes in temperature advection that might change as the planet warms, contributing to a more confident projection of future climates.

1. Introduction

Low clouds strongly cool the climate by reflecting substantial solar radiation back into space. However, they are not well simulated in climate models due to coarse resolutions and complex underlying physical processes. Enhancing our understanding of low-cloud behavior, especially marine boundary layer clouds (MBLCs), could help reduce uncertainties in climate projections (Bony & Dufresne, 2005; Cess et al., 1990; Medeiros et al., 2008; Soden & Vecchi, 2011; Vial et al., 2013; Zhang et al., 2018).

MBLCs respond strongly to changes in the meteorological environment (Stevens & Brenguier, 2009). The most well-known meteorological factor controlling MBLCs is the lower tropospheric stability (LTS; Klein & Hartmann, 1993) or the estimated inversion strength (EIS; Wood & Bretherton, 2006). A larger LTS/EIS results in more moisture trapped within the planetary boundary layer (PBL), thus increasing the MBLC fraction. Other important MBLC-controlling factors include sea surface temperature (SST), low-level temperature advection ($T_{\rm adv}$), large-scale vertical velocity, free-tropospheric (FT) relative humidity, and surface wind speed (Klein et al., 2017). These factors and their relationships with MBLC fraction help explain MBLC behavior in the present-day climate and predict their change with global warming (e.g., Brient et al., 2015; Klein et al., 2017; Myers et al., 2021; Qu et al., 2015). Among these factors, $T_{\rm adv}$'s influence on MBLCs remains the

9448007, 2023, 10, Downloaded from https:/

least understood. Cold-air advection (cold air moving over warmer SSTs) occurs globally, while warm-air advection (warm air moving over colder SSTs) is more commonly observed in mid- and high-latitudes (e.g., Myers et al., 2021; Wall et al., 2017; You et al., 2021; Zheng & Ming, 2023). Observations from two mid-latitude field campaigns, CAP-MBL (Wood et al., 2015) and MARCUS (McFarquhar et al., 2019), indicated that over 25% of single-layer stratocumulus clouds were experiencing warm-air advection (Zheng et al., 2020). There are mixed pieces of evidence regarding how MBLCs respond to changes in $T_{\rm adv}$. Some studies found the increased MBLC fraction or optical thickness as the background flow shifts from warm-air advection conditions to cold-air advection conditions (Myers & Norris, 2016; Norris & Iacobellis, 2005; Scott et al., 2020; Wall et al., 2017) while others observed no relationship (Naud et al., 2020) or even the opposite (Goren et al., 2018; Zheng & Li, 2019).

Two mechanisms were hypothesized to explain how MBLCs respond to changes in $T_{\rm adv}$. First, as $T_{\rm adv}$ increases (i.e., from cold-air to warm-air advection), the greater stabilization of the surface-atmosphere interface suppresses surface fluxes. Such a surface-atmosphere decoupling cuts off the surface moisture supply to MBLCs, so the cloudiness decreases (moisture-deficit mechanism; Klein et al., 2017; Scott et al., 2020). Second, as surface fluxes weaken, the more decoupled boundary layer entrains less effectively the FT dry air into the boundary layer. The weaker entrainment drying helps sustain the cloud decks (entrainment-drying-weakening mechanism; Zheng & Li, 2019). Which one is more dominant is central to reconciling the two seemingly contradictory mechanisms, the motivation of the current study.

We address the question using an idealized large-eddy simulation (LES) approach by decreasing the SST over a doubly periodic LES domain to mimic the influence of warm-air advection. This simulation strategy is inspired by the conventional LES approach of studying the subtropical stratocumulus-to-cumulus (Sc-to-Cu) transition (Bretherton et al., 1999; de Roode et al., 2016; Erfani et al., 2022; McGibbon & Bretherton, 2017; Sandu et al., 2010; van der Dussen et al., 2013, 2016), where the domain-averaged SST is increased to represent the role of cold-air advection. Comparing modeled MBLCs under warm- and cold-advection conditions enables singling out the control of $T_{\rm adv}$ on the clouds. Such a modeling strategy is highly idealized but can showcase the core effect of $T_{\rm adv}$. In the real world, $T_{\rm adv}$ co-varies with other synoptic meteorological variables (e.g., large-scale vertical velocity and FT moisture) so that simply varying $T_{\rm adv}$ seems unrealistic. We, however, favor such an idealized modeling strategy because our objective is to elucidate the two hypothesized mechanisms, neither of which is relevant to the coupling between $T_{\rm adv}$ and other synoptic variables. Both mechanisms are centered on the warm-advection-induced stabilization (or decoupling) of a stratocumulus-topped boundary layer (STBL), a boundary-layer scale process that is well simulated through the idealized modeling framework [see the companion paper: Zheng, Zhang, Rosenfeld, et al. (2021)]. Moreover, the elucidated mechanism by our simulations can help explain the disparity in previous observations.

2. Methodology

2.1. Model Description

The LES model used in this study is version 6.11.3 of the System for Atmospheric Modeling (SAM), provided by Marat Khairoutdinov and documented in Khairoutdinov and Randall (2003). For all simulations, a simplified (drizzle only) version of the Khairoutdinov and Kogan (2000) microphysics scheme (KK2000) was adopted for conversion between cloud and rainwater as well as raindrop evaporation and sedimentation, in which no double-moment cloud water microphysics was implemented. The cloud water droplet concentration was prescribed (Nc = 100 cm^{-3}). Tests showed that our results are not influenced by the microphysical schemes used (Text S2 in Supporting Information S1). However, these schemes do not interact with aerosols, thus not representing the positive feedback between coalescence scavenging and aerosol concentrations (Yamaguchi et al., 2017).

2.2. Experimental Design

Our cases are based on the Atlantic Stratocumulus Transition Experiment (ASTEX, Albrecht et al., 1995) first Lagrangian case, a benchmark case for LES modeling of the Sc-to-Cu transition (Bretherton et al., 1999; van der Dussen et al., 2013). During the ASTEX, an initially well-mixed boundary layer is capped by a solid stratocumulus deck that moves over an increasingly warmer sea surface. The cold-advection-induced instability of the boundary layer and the resultant enhanced cloud-top entrainment gradually thin the cloud deck, eventually breaking up the stratiform cloud, leading to shallow cumulus as the dominant cloud type (de Roode &

ZHANG ET AL. 2 of 10

19448007, 2023, 10, Downloaded from https://agupubs.onlinelibrary.viley.com/doi/10.1029/2023L101663, Wiley Online Library on [17/05/2023]. See the Terms and Conditions (https://onlinelibrary.wiley.com/terms-and-conditions) on Wiley Online Library for rules of use; OA articles are governed by the applicable Creative Commons Licensia.

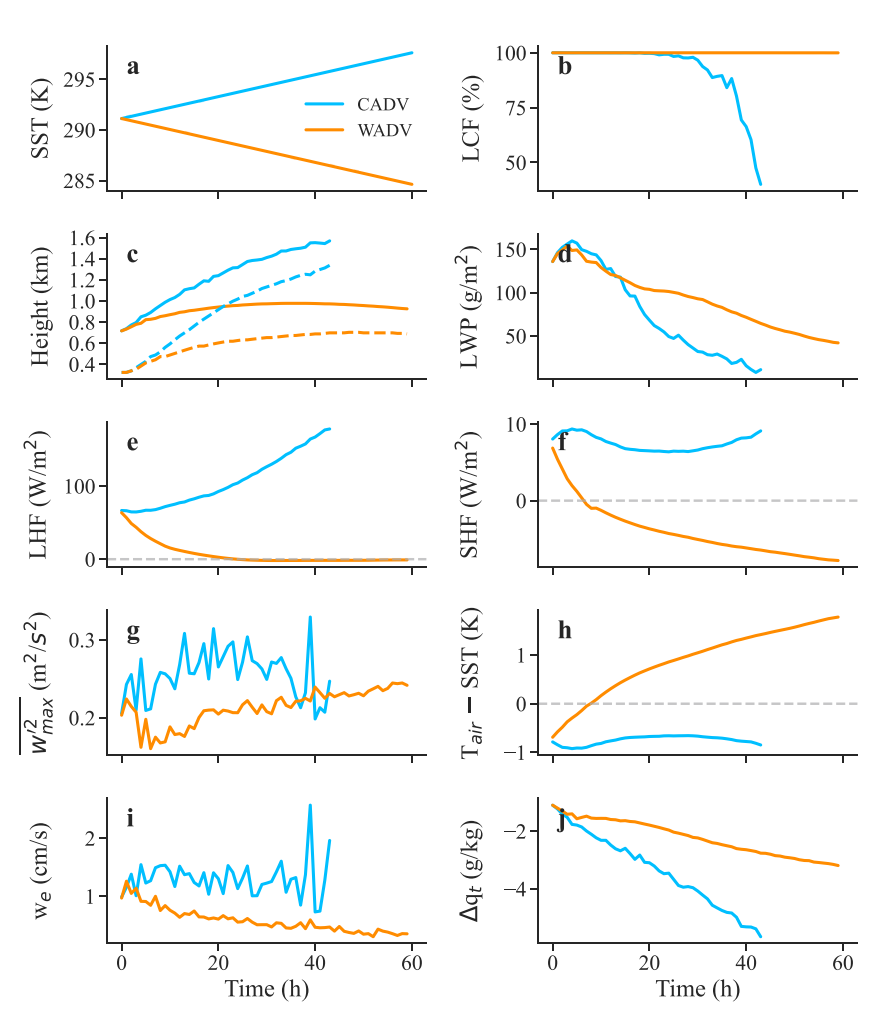


Figure 1. Time series of (a) sea surface temperature, (b) low-cloud fraction, (c) cloud-top height (solid line) and cloud-base height (dashed line), (d) liquid water path (grid-mean), (e) latent heat flux, (f) sensible heat flux, (g) maximum vertical velocity variance, (h) near-surface air temperature minus sea surface temperature, measuring the stratification degree of the surface-atmosphere interface, (i) entrainment rate at the cloud top, and (j) inversion moisture jump for experiments CADV (blue) and WADV (orange), which mimic the influence of cold-air and warm-air advection on the stratocumulus transition, respectively. Note that only the period when the calculation of cloud-base height is valid in CADV is shown for (b–j).

Duynkerke, 1997). For our cold-advection case (CADV), initial soundings and forcing conditions were similar to those used in the ASTEX LES inter-comparison project (van der Dussen et al., 2013), but with simplified forcing conditions: (a) linearizing the increasing SST time series to obtain a fixed increasing rate of 2.6 K day⁻¹; (b) averaging the diurnally varying solar zenith angle to remove the diurnal cycle influence, which is minor in our study (see Figures S10–S11 in Supporting Information S1); and (c) using a fixed large-scale divergence, D, of 5×10^{-6} s⁻¹. These simplifications do not change the main characteristics of the ASTEX cloud evolution [see the comparison figure, (Figure 1 in Zheng, Zhang, & Li, 2021)].

We generated the warm-advection case (WADV) by simply reversing the SST changing rate from 2.6 to -2.6 K/day (Figure 1a). The CADV and WADV runs imitate the influences of cold-air and warm-air advection, respectively, constituting the main simulation sets in this study. To test the robustness of our results, a series of supplementary simulations were run by varying environmental conditions (large-scale vertical velocity, cloud-top inversion strength, and FT moisture) and modeling settings (domain size, grid spacing, and cloud microphysical schemes), summarized in Table S1 in Supporting Information S1.

Each of the baseline simulations was run for 60 hr. The radiation calculation was updated every minute. These simulations were performed using a doubly periodic domain with a size of $4.2 \text{ km} \times 4.2 \text{ km}$. The horizontal resolution was 35 m. The vertical grid spacing varied from 15 m at the surface to 5 m in the height range of

ZHANG ET AL. 3 of 10

.wiley.com/doi/10.1029/2022GL101663, Wiley Online Library on [17/05/2023]. See the Terms and Condit

2.3. LWP Budget Analysis

To explore the role of physical processes in the stratocumulus evolution under warm-advection conditions, we use a budget analysis of the liquid water path (LWP) (van der Dussen et al., 2014):

$$\frac{\partial \text{LWP}}{\partial t} = \underbrace{\rho w_e \left(\eta \Delta q_t - \Pi \gamma \eta \Delta \theta_l - h \Gamma_{q_l} \right)}_{\text{Entrainment}} + \underbrace{\rho \eta \left(\overline{w' q_t'}(z_b) - \Pi \gamma \overline{w' \theta_l'}(z_b) \right)}_{\text{Cloud-base tubulent fluxes}} + \underbrace{\frac{\eta \gamma}{c_p} \cdot \left(F_{\text{rad}}(z_t) - F_{\text{rad}}(z_b) \right)}_{\text{Radiation}} + \underbrace{\left(-\rho (P(z_t) - P(z_b)) \right)}_{\text{Precipitation}} + \underbrace{\left(-\rho h \Gamma_{q_l} w_{\text{sub}}(z_i) \right)}_{\text{Subsidence}} \tag{1}$$

where ρ is the air density (kg/m³); w_e is the entrainment rate (m/s); Π is the Exner function; h is the cloud thickness (m); q_t is the total water mixing ratio (kg/kg); θ_t is the liquid water potential temperature (K); z_b is the cloudbase height (m), with z_t the cloud-top height (m); Γ_{q_t} (kg/kg/m) is the lapse rate of the liquid water mixing ratio (q_t , kg/kg); F_{rad} is the radiative flux (W/m²), and P is the precipitation flux (m/s), with both defined as negative downward; $w'q'_t(z_b)$ and $w'd'_t(z_b)$ are the moisture flux (kg/kg m/s) and the heat flux (K m/s) at the cloud base, respectively; and $w_{\text{sub}}(z_t)$ is the large-scale subsidence rate (m/s) at the top of the boundary layer, with z_t the PBL height (m). $\gamma = \frac{\partial q_s}{\partial T} \approx 0.55 \text{g/kg/K}$ is derived from the Clausius-Clapeyron relationship, with q_s the saturated specific humidity (g/kg), and η is a thermodynamic factor determined by $\left(1 + \frac{L_v \gamma}{c_p}\right)^{-1}$ where L_v is the latent heat of vapourization (J/kg), and c_p is the specific heat of air at constant pressure (J/kg/K). Δq_t and $\Delta \theta_t$ represent the inversion jump of moisture and temperature, respectively. The calculations of different heights (z_b , z_t , inversion-top height (z_t^{-1}), and inversion-base height (z_t^{-1})), inversion jumps (Δq_t and $\Delta \theta_t$), and the entrainment rate (w_e) are described in Text S1 in Supporting Information S1. Note that all variables used are slab averages.

The forcing terms on the right-hand side of Equation 1 represent the contributions of five distinct physical processes: entrainment of FT dry air into the cloud layer (*Ent*), turbulent transport of moisture and heat at the cloud base (*Base*), divergence of the net radiative flux over the cloud layer (or the effect of radiative-cooling-induced condensation, *Rad*), divergence of the precipitation flux over the cloud layer (*Prec*), and large-scale subsidence (*Subs*). *Ent*, *Prec*, and *Subs* dry the cloud layer, whereas *Rad* and *Base* moisten it.

The Ent term consists of three processes contributing to the LWP: entrainment drying $(\rho w_e \eta \Delta q_t)$, entrainment warming $(-\rho w_e \Pi \gamma \eta \Delta \theta_t)$, and cloud deepening due to entrainment $(-\rho w_e h \Gamma_{q_t})$. Intuitively, entrainment drying means that dry air from the free troposphere is entrained into the clouds and dries the clouds. The entrained dry air also tends to warm and evaporate clouds, so-called entrainment warming. Entrainment-induced cloud deepening $(-\rho w_e h \Gamma_{q_t})$ generally contributes to LWP growth, because a cloud's liquid water content at its top, where it typically reaches a maximum, increases as the cloud layer deepens due to its positive relationship with height in stratocumulus layers (Wood, 2012). The Base term has two components: moisture transport $\left[\rho \eta \overline{w'q'_t}(z_b)\right]$ and heat transport $\left[-\rho \eta \Pi \gamma \overline{w'\theta'_t}(z_b)\right]$.

3. Results

3.1. Persistence of Decoupled Stratocumulus

The stratocumulus deck in WADV maintains overcast throughout the 60-hr simulation whereas the cloud deck in CADV breaks up at $t = \sim 20$ hr (Figure 1b). The markedly longer cloud persistence simulated by LES under warm-advection conditions is qualitatively consistent with observations made by Zheng and Li (2019). The cloud breakup in CADV is expected due to the well-posed conditions for the traditional Sc-to-Cu transition framework (Bretherton & Wyant, 1997): increasing SST and surface latent heat flux (Figure 1e), a more turbulent boundary layer (Figure 1g), the emergence of cumulus penetration into the stratiform deck (Figure S3c in Supporting Information S1), and enhanced entrainment (Figure 1i). In comparison, the persistence of the cloud deck in WADV

ZHANG ET AL. 4 of 10

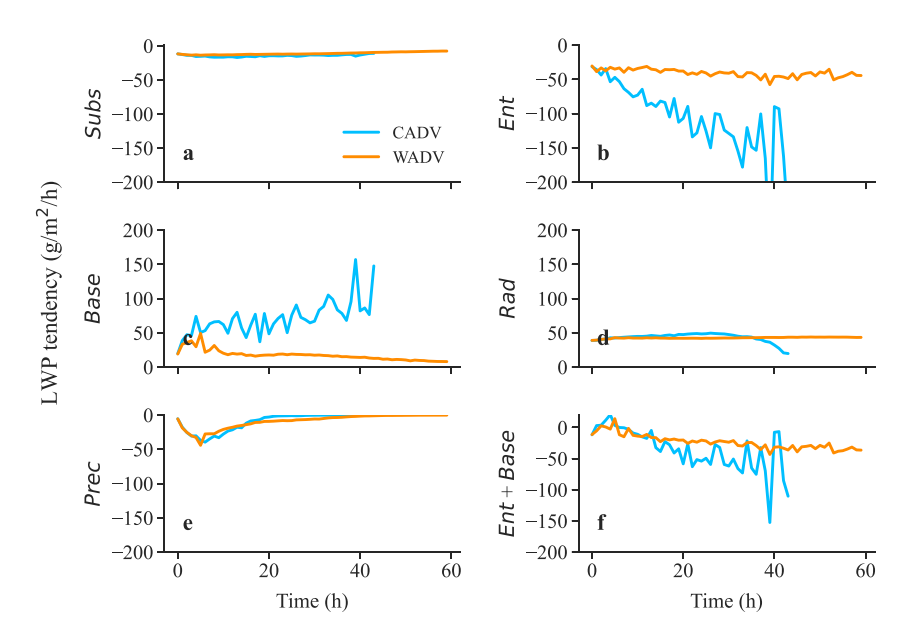


Figure 2. Time series of the LWP tendency due to (a) large-scale subsidence, (b) entrainment, (c) cloud-base turbulent fluxes, (d) radiation, and (e) precipitation for experiments CADV (blue) and WADV (orange). Panel (f) shows the combined effect of (b and c).

is less understood. The most notable feature of the WADV run, which distinguishes it from the CADV run, is the significant suppression of surface fluxes (Figures 1e and 1f) by the stable stratification of WADV (Figure 1h). Such a shut-off of energy (and moisture) influx from the ocean surface causes a complete decoupling between the stratocumulus deck and the ocean surface. Unlike Bretherton and Wyant (1997)'s "deepening-warming" decoupling that takes place in the boundary layer, this warm-advection-induced decoupling primarily occurs at the surface-atmosphere interface [see more differences in Zheng, Zhang, Rosenfeld, et al. (2021)], and such a surface-atmosphere decoupling can be measured by near-surface inversion strength (Figure 1h). The decoupling has two consequences related to the moisture-deficit mechanism and the entrainment-drying-weakening mechanism, discussed in the Introduction. First, the decoupling cuts off the surface moisture supply to the clouds. With limited moisture supply from the ocean, the cloud deck gradually thins (Figure 1c) and the cloud LWP continuously decreases over time (Figure 1d). Second, the turbulent intensity in a strongly decoupled STBL is lower than its weakly decoupled counterpart in CADV (Figures 1g and 1h), so entrainment is considerably weaker (Figure 1i). The weaker entrainment drying buffers the cloud decaying.

Assuming no other mechanism at work, the net consequence of these two mechanisms is to prolong the lifetime of stratocumulus decks in WADV, compared with that in CADV. Despite the shut-off of the surface moisture supply by decoupling, the reduced entrainment drying buffers the system, preventing the emergence of a nonlinear run-away effect that may cause the stratiform cloud deck to break up rapidly, as experienced by the cloud regime transition under cold-advection conditions (Wyant et al., 1997). Such a conclusion is never complete without the following questions being answered. Are there other mechanisms contributing? If not, can we quantify the impacts of these two mechanisms to solidify the conclusion? How does the result depend on environmental conditions? We address these questions using an LWP budget decomposition approach in the next section.

3.2. LWP Budget Analysis

The LWP budget analysis allows decomposing the temporal change of cloud LWP into the five individual tendency terms: two source terms (cloud-base moisture flux and cloud-layer radiative cooling) and three sink terms (entrainment, precipitation, and large-scale subsidence). The influences of the relevant physical processes on the LWP changes are examined in this section. Note that closure between the simulated LWP tendency and the sum of the budget terms is checked in Figure S4 in Supporting Information S1, and the unclosed case is only noticed in CADV after cloud dissipation starts, indicating that there might be other processes controlling the LWP not considered here. Figure 2 compares the evolutions of the five terms between WADV and CADV. The

ZHANG ET AL. 5 of 10

most noticeable differences between the two runs are the markedly smaller *Base* and less negative *Ent* in WADV than in CADV. Other terms are similar between the two runs, suggesting that no other mechanisms contribute to the LWP difference. This finding points to changes in *Base* and *Ent* as the two dominant mechanisms that control the LWP difference between WADV and CADV. As such, we take a closer look at these two terms.

We first examine the *Base* term. It is positive in either run (Figure 2c) because turbulence transports moist air from the sea surface that cools down to be condensed, adding liquid water into cloud layers and raising the LWP. In WADV, due to the lack of surface fluxes (Figures 1e and 1f), cloud-top longwave radiative cooling becomes the sole driver of PBL turbulence, yielding a much smaller Base term than that in CADV. The Base term consists of two components representing moisture transport ($Base_q$) and heat transport ($Base_h$). Figure S5 in Supporting Information S1 shows their evolution. The $Base_q$ term dominates in both runs but becomes significantly smaller in WADV. In summary, the Base term is significantly decreased in WADV, mostly due to the moisture transport component.

If only the *Base* term was considered, the LWP would dissipate more rapidly in WADV than in CADV. However, the change in *Ent* buffers the dissipation. Figure 2b shows that the effect of the entrainment-induced cloud dissipation is much weaker in WADV than in CADV. To understand the physics of the decrease, we further decompose the *Ent* term into three components: entrainment drying (Ent_q) , entrainment warming (Ent_h) , and entrainment-induced cloud deepening (Ent_z) . In either run, the cloud-deepening effect on the LWP is notably lower than the other two effects (Figure S6c in Supporting Information S1), especially late in the simulations. In CADV, the entrainment drying effect dominates the LWP consumption, followed by the entrainment warming effect (Figures S6a and S6b in Supporting Information S1). However, both effects are greatly reduced in WADV (particularly the drying effect owing to a large decrease in the moisture jump strength, Figure 1j), which helps maintain the LWP.

The combined effect of changes in *Base* and *Ent* is to prolong the lifetime of clouds in WADV, compared to CADV. Figure 2f shows that the magnitude of *Base* + *Ent* is smaller in WADV, indicating that the cloud-favoring effect due to the reduction in entrainment drying (the entrainment-drying-weakening mechanism) is more significant than the cloud-reducing effect induced by the concomitant moisture deficit (the moisture-deficit mechanism) under warm-advection conditions. This explains well why the cloud fraction and cloud LWP are maintained much longer under warm-advection than under cold-advection conditions.

3.3. Environmental Dependence

We have shown that warm-advection-induced decoupling helps prolong the lifetime of the stratocumulus deck because of the much weaker entrainment than that in CADV. Such a cloud-sustaining effect by the decreased entrainment outweighs the cloud-reducing effect by the reduced cloud-base moisture flux. Is this finding (i.e., decoupling-induced cloud-prolonging effect) valid for different large-scale environments? We tested the environmental impact by perturbing several well-known environmental quantities (i.e., large-scale vertical velocity, cloud-top inversion strength, and FT moisture). It holds well (Figures S7–S9 in Supporting Information S1) although the degree of the prolonging effect varies. The impact of FT moisture merits discussion here because its impact on cloud lifetime is closely tied to the surface-atmosphere decoupling, a key concept central to this study. We varied FT moisture by -10%, -5%, 5%, and 10% in WADV and CADV (Figure S12 in Supporting Information S1) to generate two sets of experiments (named WADV_FTMs and CADV_FTMs, respectively). To quantify the cloud lifetime, we use the e-folding time of LWP (τ), which describes the timescale of LWP to decrease to 1/e of its initial value.

Figure 3a shows the variation in τ with changes in FT moisture (gray lines). As expected, τ increases with FT moisture for both WADV_FTMs and CADV_FTMs. However, the sensitivity differs: The cloud-prolonging effect of FT moisture is more pronounced under warm-advection than cold-advection conditions. This is more clearly seen in Figure 3b, showing the difference in τ between WADV_FTMs and CADV_FTMs, denoted as $\Delta_{\rm adv}\tau$, where the " $\Delta_{\rm adv}$ " means WADV minus CADV. What causes this difference in the sensitivity? The main reason is the contrast between the WADV and CADV cloud-surface coupling states. In CADV, the cloud-deck breakup is well known to be driven by increasing surface latent heat fluxes that enhance entrainment drying (Bretherton & Wyant, 1997; Zheng, Zhang, & Li, 2021). Higher humidity in the free troposphere (or reduced cloud-top radiative cooling) can delay the breakup (gray dashed line in Figure 3a) but does not fundamentally

ZHANG ET AL. 6 of 10

19448007, 2023, 10, Downloaded from https://agupubs.onlinelibrary.wiley.com/doi/10.1029/2022GL101663, Wiley Online Library on [17/05/2023]. See the Terms and Conditions (https://

ditions) on Wiley Online Library for rules of use; OA articles are governed by the applicable Creative Commons License

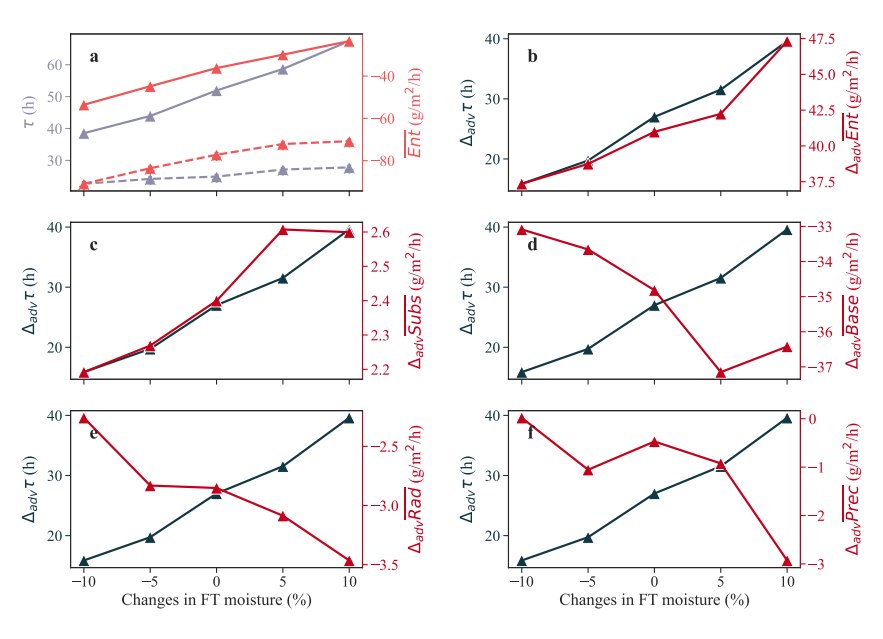


Figure 3. (a) The e-folding time of liquid water path (τ, gray) and the mean LWP tendency due to entrainment over the cloud lifetime $(\overline{Ent}, \text{ light red})$ as a function of percentage changes in the free-tropospheric (FT) moisture (compared to control experiments) for experiments WADV_FTMs (solid line) and CADV_FTMs (dashed line). (b) Differences in τ (black) and \overline{Ent} (red) between experiments WADV_FTMs and CADV_FTMs as a function of the change in FT moisture. Panels (c-f) are the same as (b), but for the large-scale subsidence term (Subs), the cloud-base turbulent flux term (Base), the radiation term (Rad), and the precipitation term (Prec), respectively.

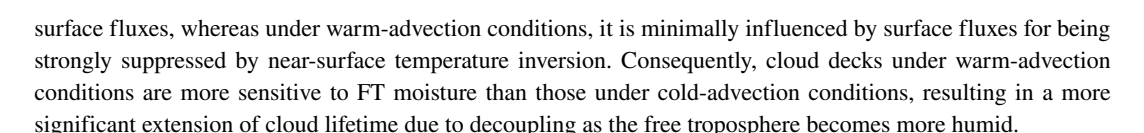
change the mechanism that the enhanced surface forcing is the dominant driver of cloud breakup as opposed to FT forcing. In WADV, however, the cloud deck is decoupled from surface fluxes. Without the dynamic control of surface forcing, the strength of entrainment drying is more closely tied to the humidity of the overlying FT air.

The above argument is reinforced by looking at the strength of entrainment drying, \overline{Ent} (the overbar means the average over the cloud lifetime). As shown by the light red lines in Figure 3a, \overline{Ent} decreases, in absolute value, with FT moisture, consistent with the role of FT moistening in weakening entrainment drying via reducing the moisture jump across cloud tops. But the decrease in entrainment drying strength is more pronounced for WADV_FTMs than CADV_FTMs, as seen $\underline{from} \Delta_{adv} \overline{Ent}$ (red line) in Figure 3b. The good alignment in the shape of the relationship between $\Delta_{adv} \tau$ and $\Delta_{adv} \overline{Ent}$ (Figure 3b) supports our argument that the decoupling-induced larger sensitivity of entrainment drying to FT moisture in WADV is the main cause for the more prolonged cloud lifetime by FT moistening. Other cloud budget terms are also examined (Figure 3c-3f), showing that adjustments in Base, Rad, and Prec make notably negative contributions to prolonging cloud lifetime, counterbalancing most of the Ent effect. Among them, the Base adjustment has the largest negative contribution due to reduced turbulent mixing in response to FT moistening (or weakened cloud-top radiative cooling).

4. The Mechanisms and Relevance to Observed Relationships

Given the same initial conditions, our simulation results demonstrate that cloud decks under warm-advection conditions live longer than their cold counterparts, because the entrainment-drying-weakening mechanism outweighs the moisture-deficit mechanism. When an initially overcast stratocumulus deck moves over warmer water, the latent-heat-flux induced entrainment drying becomes increasingly stronger, leading to the breakup of cloud layers, a classical phenomenon of stratocumulus-to-cumulus transition (Bretherton & Wyant, 1997; Krueger et al., 1995). However, when the same cloud deck moves over colder water, it lasts longer due to stabilization (or decoupling) of the surface-atmosphere interface by warm-air advection, which weakens both PBL turbulence and cloud-top entrainment. The cloud-favoring mechanism of weaker entrainment dominates the cloud-reducing mechanism of decoupling-induced reduction in surface moisture supply, thereby prolonging cloud persistence. This longer persistence of cloud fraction and LWP is more pronounced with higher FT humidity (i.e., reduced cloud-top radiative cooling). Under cold-advection conditions, the entrainment drying is primarily driven by

ZHANG ET AL. 7 of 10



How is the mechanism relevant to observations of MBLC-T_{adv} relationships? According to the mechanism, the warm-advection-induced decoupling makes the stratocumulus deck persist longer. This is consistent with Zheng and Li (2019)'s work, in which they used a geostationary satellite to track the evolution of initially overcast stratocumulus decks, finding that WADV can help prolong the cloud lifetime. However, why do many observational studies show the opposite (e.g., Myers & Norris, 2016; Norris & Iacobellis, 2005; Scott et al., 2020)? It is likely because of the use of the conventional Eulerian analysis method, which correlates the instantaneous cloud properties with $T_{\rm adv}$ at fixed locations. Unlike Zheng and Li (2019)'s Lagrangian approach that starts with a preexisting cloud deck, the Eulerian framework collects all air masses regardless of their histories and initial states. Warm-advection events typically occur in the warm sections of extra-tropical cyclones. These regions are characterized by large-scale ascending motions and a relatively unstable troposphere (compared to cold sections), neither favoring the formation of overcast solid stratiform decks (Wood, 2012). As such, under warm-advection conditions, MBLCs have low cloud coverages at their births. In this regard, the cloud fraction must be lower in warm-advection flows since they start with low cloudiness already. In other words, there are not enough overcast stratocumulus sheets for the aforementioned mechanism to operate upon. This helps explain why Eulerian-method-based studies tend to observe a negative MBLC-T_{adv} correlation. In summary, a warm-advection-related environment does not favor the formation of stratocumulus sheets. But once stratocumulus forms (or is advected from different environments), the warm-advection condition and the resultant surface-atmosphere decoupling help sustain its persistency.

5. Summary

There have been mixed observation-based findings in regard to the impact of warm-air advection upon marine stratocumulus lifetime (Goren et al., 2018; Myers & Norris, 2016; Naud et al., 2020; Norris & Iacobellis, 2005; Scott et al., 2020; Wall et al., 2017; Zheng & Li, 2019). In this study, we carried out idealized large-eddy simulations to elucidate this problem. Warm-air advection was mimicked by decreasing the sea surface temperature linearly in a doubly periodic domain. Our simulation results show that under warm-advection conditions stratocumulus clouds can last significantly longer than under cold-advection conditions assuming identical initial conditions. This cloud-prolonging effect by warm-air advection is caused by the warm-advection-induced stabilization/decoupling of the surface-atmosphere interface that weakens cloud-top entrainment drying. Such a cloud-favoring effect by reduced entrainment drying is more significant than the cloud-reducing effect due to reduced moisture supply from the ocean by decoupling. By perturbing environmental factors typical for midlatitude regions (e.g., subsidence, cloud-top inversion strength, and free-tropospheric moisture), we find that our results hold well (Figures S7–S9 in Supporting Information S1). One potential limit of our study is that it may not apply to real-world regimes with very dry free-tropospheric backgrounds as our simulations cannot produce clouds under such conditions. Also, our study is based on the ASTEX case where the drizzle is weak, so in the regime where precipitation is ubiquitous, like those shown in Zhu et al. (2022), suppression of precipitation under warm-advection conditions may have a greater impact on prolonging LWP than the reduction in entrainment drying. Finally, the effects of aerosols on cloud evolution are potentially important (Erfani et al., 2022), which were not included here. These limitations could be addressed in the future by running realistic LES simulations when Lagrangian observations of stratocumulus decks experiencing warm-air advection are available.

Data Availability Statement

The SAM model code is available at http://rossby.msrc.sunysb.edu/~marat/SAM.html. All simulation data are available at https://doi.org/10.5281/zenodo.7478642.

ZHANG ET AL. 8 of 10



Acknowledgments

This study is supported by the Department of Energy (DOE) Atmospheric System Research program (DESC0022919), the National Science Foundation (AGS2126098), and the National Research Foundation of Korea (NRF) grant funded by the Korean government (MSIT) (No. NRF2020R1A2C1003215 and NRF2023R1A2C1002367). The authors acknowledge the University of Maryland supercomputing resources (http://hpcc. umd.edu) made available for conducting the research reported in this paper. The authors thank Marat Khairoutdinov for maintaining the SAM code and Peter Blossey for help in setting up the ASTEX case. The authors thank Michael Diamond and two anonymous reviewers for their constructive comments, which considerably improve the quality of the manuscript, and Maureen Cribb for editing this manuscript.

References

- Albrecht, B. A., Bretherton, C. S., Johnson, D., Scubert, W. H., & Frisch, A. S. (1995). The Atlantic stratocumulus transition experiment—ASTEX. Bulletin of the American Meteorological Society, 76(6), 889–904. https://doi.org/10.1175/1520-0477(1995)076<0889:TASTE>2. 0.CO:2
- Bony, S., & Dufresne, J.-L. (2005). Marine boundary layer clouds at the heart of tropical cloud feedback uncertainties in climate models. Geophysical Research Letters, 32(20), 1–4. https://doi.org/10.1029/2005GL023851
- Bretherton, C. S., Krueger, S. K., Wyant, M. C., Bechtold, P., Van Meijgaard, E., Stevens, B., & Teixeira, J. (1999). A GCSS boundary-layer cloud model intercomparison study of the first ASTEX Lagrangian experiment. *Boundary-Layer Meteorology*, 93(3), 341–380. https://doi. org/10.1023/A:1002005429969
- Bretherton, C. S., & Wyant, M. C. (1997). Moisture transport, lower-tropospheric stability, and decoupling of cloud-topped boundary layers. Journal of the Atmospheric Sciences, 54(1), 148–167. https://doi.org/10.1175/1520-0469(1997)054<0148:MTLTSA>2.0.CO;2
- Brient, F., Schneider, T., Tan, Z., Bony, S., Qu, X., & Hall, A. (2015). Shallowness of tropical low clouds as a predictor of climate models? Response to warming. Climate Dynamics, 47(1–2), 433–449. https://doi.org/10.1007/s00382-015-2846-0
- Cess, R. D., Potter, G. L., Blanchet, J. P., Boer, G. J., Del Genio, A. D., Deque, M., et al. (1990). Intercomparison and interpretation of climate feedback processes in 19 atmospheric general circulation models. *Journal of Geophysical Research*, 95(D10), 16601–16615. https://doi.org/10.1029/jd095id10p16601
- De Roode, S. R., & Duynkerke, P. G. (1997). Observed Lagrangian transition of stratocumulus into cumulus during ASTEX: Mean state and turbulence structure. *Journal of the Atmospheric Sciences*, 54(17), 2157–2173. https://doi.org/10.1175/1520-0469(1997)054<2157:OLTOSI>2.0.CO:2
- de Roode, S. R., Sandu, I., van der Dussen, J. J., Ackerman, A. S., Blossey, P., Jarecka, D., et al. (2016). Large eddy simulations of EUCLIPSE/GASS Lagrangian stratocumulus to cumulus transitions: Mean state, turbulence, and decoupling. *Journal of the Atmospheric Sciences*, 73(6), 2485–2508. https://doi.org/10.1175/jas-d-15-0215.1
- Erfani, E., Blossey, P., Wood, R., Mohrmann, J., Doherty, S. J., Wyant, M., & Kuan-Ting, O. (2022). Simulating aerosol lifecycle impacts on the subtropical stratocumulus-to-cumulus transition using large-eddy simulations. *Journal of Geophysical Research: Atmospheres*, 127(21), e2022JD037258. https://doi.org/10.1029/2022JD037258
- Goren, T., Rosenfeld, D., Sourdeval, O., & Quaas, J. (2018). Satellite observations of precipitating marine stratocumulus show greater cloud fraction for decoupled clouds in comparison to coupled clouds. Geophysical Research Letters, 45(10), 5126–5134. https://doi. org/10.1029/2018GL078122
- Khairoutdinov, M., & Kogan, Y. (2000). A new cloud physics parameterization in a large-eddy simulation model of marine stratocumulus. Monthly Weather Review, 128(1), 229–243. https://doi.org/10.1175/1520-0493(2000)128<0229:ancppi>2.0.co;2
- Khairoutdinov, M. F., & Randall, D. A. (2003). Cloud resolving modeling of the ARM summer 1997 IOP: Model formulation, results, uncertainties, and sensitivities. *Journal of the Atmospheric Sciences*, 60(4), 607–625. https://doi.org/10.1175/1520-0469(2003)060<0607:crmota>2.0.co;2
- Klein, S. A., Hall, A., Norris, J. R., & Pincus, R. (2017). Low-cloud feedbacks from cloud-controlling factors: A Review. Surveys in Geophysics, 38(6), 1307–1329. https://doi.org/10.1007/s10712-017-9433-3
- Klein, S. A., & Hartmann, D. L. (1993). The seasonal cycle of low stratiform clouds. *Journal of Climate*, 6(8), 1587–1606. https://doi.org/10.1175/1520-0442(1993)006<1587:TSCOLS>2.0.CO:2
- Krueger, S. K., McLean, G. T., & Fu, Q. (1995). Numerical simulation of the stratus-to-cumulus transition in the subtropical marine boundary layer. Part II: Boundary-layer circulation. *Journal of the Atmospheric Sciences*, 52(16), 2851–2868. https://doi. org/10.1175/1520-0469(1995)052<2851:NSOTST>2.0.CO;2
- McFarquhar, G., Marchand, R., Bretherton, C., Alexander, S., Protat, A., Siems, S., et al. (2019). Measurements of aerosols, radiation, and clouds over the southern ocean (MARCUS) field campaign report.
- McGibbon, J., & Bretherton, C. S. (2017). Skill of ship-following large-eddy simulations in reproducing MAGIC observations across the northeast Pacific stratocumulus to cumulus transition region. *Journal of Advances in Modeling Earth Systems*, 9(2), 810–831. https://doi.org/10.1002/2017MS000924
- Medeiros, B., Stevens, B., Held, I. M., Zhao, M., Williamson, D. L., Olson, J. G., & Bretherton, C. S. (2008). Aquaplanets, climate sensitivity, and low clouds. *Journal of Climate*, 21(19), 4974–4991. https://doi.org/10.1175/2008jcli1995.1
- Myers, T. A., & Norris, J. R. (2016). Reducing the uncertainty in subtropical cloud feedback. *Geophysical Research Letters*, 43(5), 2144–2148. https://doi.org/10.1002/2015GL067416
- Myers, T. A., Scott, R. C., Zelinka, M. D., Klein, S. A., Norris, J. R., & Caldwell, P. M. (2021). Observational constraints on low cloud feedback reduce uncertainty of climate sensitivity. *Nature Climate Change*, 11(6), 501–507. https://doi.org/10.1038/s41558-021-01039-0
- Naud, C. ~M., Booth, J. ~F., Protat, A., Lamer, K., Marchand, R., & McFarquhar, G. ~M. (2020). Boundary layer cloud controlling factors in the midlatitudes: Southern versus Northern Ocean Clouds. *AGU Fall Meeting Abstracts*, 2020, A195-02.
- Norris, J. R., & Iacobellis, S. F. (2005). North Pacific cloud feedbacks inferred from synoptic-scale dynamic and thermodynamic relationships. *Journal of Climate*, 18(22), 4862–4878. https://doi.org/10.1175/JCL13558.1
- Qu, X., Hall, A., Klein, S. A., & Deangelis, A. M. (2015). Positive tropical marine low-cloud cover feedback inferred from cloud-controlling factors. Geophysical Research Letters, 42(18), 7767–7775. https://doi.org/10.1002/2015GL065627
- Sandu, I., Stevens, B., & Pincus, R. (2010). On the transitions in marine boundary layer cloudiness. *Atmospheric Chemistry and Physics*, 10(5), 2377–2391. https://doi.org/10.5194/acp-10-2377-2010
- Scott, R. C., Myers, T. A., Norris, J. R., Zelinka, M. D., Klein, S. A., Sun, M., & Doelling, D. R. (2020). Observed sensitivity of low-cloud radiative effects to meteorological perturbations over the global oceans. *Journal of Climate*, 33(18), 7717–7734. https://doi.org/10.1175/JCLI-D-19-1028.1
- Soden, B. J., & Vecchi, G. A. (2011). The vertical distribution of cloud feedback in coupled ocean-atmosphere models. Geophysical Research Letters, 38(12), L12704. https://doi.org/10.1029/2011GL047632
- Stevens, B., & Brenguier, J. L. (2009). Cloud controlling factors: Low clouds. In J. Heintzenberg & R. J. Charlson (Eds.), Clouds in the perturbed climate system. MIT Press.
- van der Dussen, J. J., de Roode, S. R., Ackerman, A. S., Blossey, P. N., Bretherton, C. S., Kurowski, M. J., et al. (2013). The GASS/EUCLIPSE model intercomparison of the stratocumulus transition as observed during ASTEX: LES results. *Journal of Advances in Modeling Earth Systems*, 5(3), 483–499. https://doi.org/10.1002/jame.20033
- van der Dussen, J. J., de Roode, S. R., & Siebesma, A. P. (2014). Factors controlling rapid stratocumulus cloud thinning. *Journal of the Atmospheric Sciences*, 71(2), 655–664. https://doi.org/10.1175/JAS-D-13-0114.1

ZHANG ET AL. 9 of 10



Geophysical Research Letters

- 10.1029/2022GL101663
- van der Dussen, J. J., de Roode, S. R., & Siebesma, A. P. (2016). How large-scale subsidence affects stratocumulus transitions. *Atmospheric Chemistry and Physics*, 16(2), 691–701. https://doi.org/10.5194/acp-16-691-2016
- Vial, J., Dufresne, J.-L., & Bony, S. (2013). On the interpretation of inter-model spread in CMIP5 climate sensitivity estimates. Climate Dynamics, 41(11–12), 3339–3362. https://doi.org/10.1007/s00382-013-1725-9
- Wall, C. J., Hartmann, D. L., & Ma, P. L. (2017). Instantaneous linkages between clouds and large-scale meteorology over the Southern Ocean in observations and a climate model. *Journal of Climate*, 30(23), 9455–9474. https://doi.org/10.1175/JCLI-D-17-0156.1
- Wood, R. (2012). Stratocumulus clouds. Monthly Weather Review, 140(8), 2373-2423. https://doi.org/10.1175/MWR-D-11-00121.1
- Wood, R., & Bretherton, C. S. (2006). On the relationship between stratiform low cloud cover and lower-tropospheric stability. *Journal of Climate*, 19(24), 6425–6432. https://doi.org/10.1175/JCLI3988.1
- Wood, R., Wyant, M., Bretherton, C. S., Rémillard, J., Kollias, P., Fletcher, J., et al. (2015). Clouds, aerosols, and precipitation in the marine boundary layer: An arm mobile facility deployment. *Bulletin of the American Meteorological Society*, 96(3), 419–439. https://doi.org/10.1175/ BAMS-D-13-00180.1
- Wyant, M. C., Bretherton, C. S., Rand, H. A., & Stevens, D. E. (1997). Numerical simulations and a conceptual model of the stratocumulus to trade cumulus transition. *Journal of the Atmospheric Sciences*, 54(1), 168–192. https://doi.org/10.1175/1520-0469(1997)054<0168:NSAACM>2.0.CO;2
- Yamaguchi, T., Feingold, G., & Kazil, J. (2017). Stratocumulus to cumulus transition by drizzle. *Journal of Advances in Modeling Earth Systems*, 9(6), 2333–2349. https://doi.org/10.1002/2017ms001104
- You, C., Tjernström, M., & Devasthale, A. (2021). Warm-air advection over melting sea-ice: A Lagrangian case study. Boundary-Layer Meteorology, 179(1), 99–116. https://doi.org/10.1007/s10546-020-00590-1
- Zhang, H., Wang, M., Guo, Z., Zhou, C., Zhou, T., Qian, Y., et al. (2018). Low-cloud feedback in CAM5 CLUBB: Physical mechanisms and parameter sensitivity analysis. *Journal of Advances in Modeling Earth Systems*, 10(11), 1–21. https://doi.org/10.1029/2018MS001423
- Zheng, Y., & Li, Z. (2019). Episodes of warm-air advection causing cloud-surface decoupling during the MARCUS. *Journal of Geophysical Research: Atmospheres*, 124(22), 12227–12243. https://doi.org/10.1029/2019jd030835
- Zheng, Y., & Ming, Y. (2023). Low-level cloud budgets across sea ice edges. Journal of Climate, 36(1), 3-18. https://doi.org/10.1175/
- Zheng, Y., Rosenfeld, D., & Li, Z. (2020). A more general paradigm for understanding the decoupling of stratocumulus-topped boundary layers: The importance of horizontal temperature advection. Geophysical Research Letters, 47(14), e2020GL087697. https://doi.org/10.1029/2020g1087697
- Zheng, Y., Zhang, H., & Li, Z. (2021). Role of surface latent heat flux in shallow cloud transitions: A mechanism-denial LES study. *Journal of the Atmospheric Sciences*, 2709–2723. https://doi.org/10.1175/JAS-D-20-0381.1
- Zheng, Y., Zhang, H., Rosenfeld, D., Lee, S.-S., & Li, Z. (2021a). Idealized large-eddy simulations of stratocumulus advecting over cold water. Part I: Boundary layer decoupling. *Journal of the Atmospheric Sciences*, 78(12), 4089–4102. https://doi.org/10.1175/JAS-D-21-0108.1
- Zhu, Z., Kollias, P., Luke, E., & Yang, F. (2022). New insights on the prevalence of drizzle in marine stratocumulus clouds based on a machine learning algorithm applied to radar Doppler spectra. Atmospheric Chemistry and Physics, 22(11), 7405–7416. https://doi.org/10.5194/ acp-22-7405-2022

References From the Supporting Information

- Hersbach, H., Bell, B., Berrisford, P., Hirahara, S., Horányi, A., Muñoz-Sabater, J., et al. (2020). The ERA5 global reanalysis. *Quarterly Journal of the Royal Meteorological Society*, 146(730), 1999–2049. https://doi.org/10.1002/qj.3803
- Minnis, P., Sun-Mack, S., Chen, Y., Chang, F. L., Yost, C. R., Smith, W. L., et al. (2021). CERES MODIS cloud product retrievals for Edition 4 Part I: Algorithm changes. *IEEE Transactions on Geoscience and Remote Sensing*, 59(4), 2744–2780. https://doi.org/10.1109/TCBS.2020.2008866
- Morrison, H., & Milbrandt, J. A. (2015). Parameterization of cloud microphysics based on the prediction of bulk ice particle properties. Part I: Scheme description and idealized tests. *Journal of the Atmospheric Sciences*, 72(1), 287–311. https://doi.org/10.1175/JAS-D-14-0065.1
- Morrison, H., Curry, J. A., & Khvorostyanov, V. I. (2005). A new double-moment microphysics parameterization for application in cloud and climate models. Part I: Description. *Journal of the Atmospheric Sciences*, 62(6), 1665–1677. https://doi.org/10.1175/JAS3446.1
- Thompson, G., Field, P. R., Rasmussen, R. M., & Hall, W. D. (2008). Explicit forecasts of winter precipitation using an improved bulk microphysics scheme. Part II: Implementation of a new snow parameterization. *Monthly Weather Review*, 136(12), 5095–5115. https://doi.org/10.1175/2008MWR2387.1
- Yamaguchi, T., & Randall, D. A. (2008). Large-eddy simulation of evaporatively driven entrainment in cloud-topped mixed layers. *Journal of the Atmospheric Sciences*, 65(5), 1481–1504. https://doi.org/10.1175/2007JAS2438.1